Dynamical evolution of a magnetic field in the preequilibrium quark-gluon plasma

Li Yan[1,2,*] and Xu-Guang Huang[3,2,†]

[1]Institute of Modern Physics, Fudan University, Shanghai 200433, China
[2]Key Laboratory of Nuclear Physics and Ion-beam Application (MOE), Fudan University, Shanghai 200433, China
[3]Physics Department and Center for Particle Physics and Field Theory, Fudan University, Shanghai 200438, China

(Received 19 April 2021; revised 15 November 2021; accepted 4 May 2023; published 23 May 2023)

High-energy heavy-ion collisions generate an extremely strong magnetic field which plays a key role in a number of novel quantum phenomena in quark-gluon plasma (QGP), such as the chiral magnetic effect. However, due to the complexity in theoretical modelings of the coupled electromagnetic fields and the QGP system, especially in the preequilibrium stages, the lifetime of the magnetic field in the QGP medium remains undetermined. We establish, for the first time, a kinetic framework to study the dynamical decay of the magnetic field in the early stages of a weakly coupled QGP by solving the coupled Boltzmann and Maxwell equations. We find that at late times a magnetohydrodynamical description of the coupled system emerges. With respect to realistic collisions at RHIC and the LHC, we estimate the residual strength of the magnetic field in the QGP when the system starts to evolve hydrodynamically.

DOI: 10.1103/PhysRevD.107.094028

I. INTRODUCTION

Quantum chromodynamics (QCD), the modern theory of strong interaction, predicts that at a sufficiently high temperature, quarks and gluons are liberated from hadrons and form a new state of matter—the quark-gluon plasma (QGP). Creating and investigating QGP is the main purpose of the BNL relativistic heavy ion collider (RHIC) and one of the main purposes of the CERN Large Hadron Collider (LHC). In these experiments, due to the relativistic motion of ions and the smallness of the colliding systems, extremely strong magnetic fields (with peak strength $|eB| \sim 10^{19}$ G at RHIC and $\sim 10^{20}$ G at the LHC) are generated [1–5]. Strong magnetic fields can significantly influence QGP and drive a number of interesting quantum phenomena [6–18]. One famous example is the chiral magnetic effect (CME), which provides a feasible means to monitor the topological fluctuations of QCD in high-temperature environments [6,7]. However, theoretical studies on such phenomena suffer from considerable uncertainties due to the lack of knowledge on the dynamical evolution of the magnetic fields in QGP. Especially, the lifetime of these fields, which essentially relies on how they decay along with the QGP evolution, remains unknown.

Shortly after the nucleus-nucleus collisions, the created magnetic fields start to decay drastically due to the departure of the Lorentz contracted nuclei from the colliding zone, inducing strong electric fields in the QGP. It is a theoretical challenge to consistently describe the subsequent evolution of the coupled electromagnetic (EM) fields and QGP. Efforts have been provoked assuming a fully thermalized QGP with charge conductivity of the QGP as input, either solving Maxwell equations or based on magnetohydrodynamics (MHD) [19–26], indicating that induction in a QGP fluid indeed slows down the decay of the magnetic fields. However, the *dominant* effects on the decay of magnetic fields from the very early stages, in which the magnetic fields decay most violently and the QGP is highly out of equilibrium, have not been discussed so far.

It is the purpose of this paper to perform a consistent computation of the dynamical evolution of EM fields in the preequilibrium QGP. We will establish a framework that based on a kinetic description for a weakly coupled QGP system, i.e., assuming the strong coupling constant α_s to be small, and the Maxwell equations for the evolution of the EM fields. Since the kinetic description has been applied extensively to analyzing the onset of hydrodynamics in QGP [27–29], it is also our interest to investigate the emergence of MHD from the QCD plasma, in the presence of dynamically evolving EM fields.

II. FORMULATION OF THE ELECTROMAGNETIC FIELD IN QGP

We start from the coupled equations that consist of the Maxwell equations that determine the dynamical evolution

*cliyan@fudan.edu.cn
†huangxuguang@fudan.edu.cn

of the EM fields and a Boltzmann equation that determines the evolution of QGP,

$$\partial_\mu F^{\mu\nu} = j^\nu_{\rm ex} + j^\nu_{\rm ind}, \tag{1a}$$

$$[p^\mu \partial_\mu + eQ_a p_\mu F^{\mu\nu}\partial_{p^\nu}] f_a(t,\mathbf{x},\mathbf{p}) = \mathcal{C}[f_a]. \tag{1b}$$

In these equations, $F^{\mu\nu} = \partial^\mu A^\nu - \partial^\nu A^\mu$ is the EM-field strength tensor and f_a is the distribution function of QGP constituents, viz. $a = q, \bar{q}$, or g for quark, antiquark, or gluon, with Q_a being the corresponding charge number.

The couplings between the EM fields and QGP are formulated in Eqs. (1) in a complex way. For the EM fields, it is self-consistently introduced through the induced charge current,

$$j^\mu_{\rm ind} = e\sum Q_q \int \frac{d^3\mathbf{p}}{(2\pi)^3}\frac{p^\mu}{E_q} h_q(t,\mathbf{x},\mathbf{p}), \tag{2}$$

where we have defined the splitting distribution $h_q \equiv f_q - f_{\bar{q}}$ to characterize the deviation between quark and antiquark distributions due to the presence of EM fields. The summation in Eq. (2) is over spin, flavor ($N_f = 2$), and color ($N_c = 3$). In addition to $j^\mu_{\rm ind}$, in heavy-ion collisions there is also an external charged current, $j^\mu_{\rm ex}$, generated by the moving spectators of the colliding nucleus, whose evolution is independent of the QGP medium. On the other hand, for quarks, the couplings are represented via the Coulomb-Lorentz force in Eq. (1b). Note, however, gluons do not directly couple to the EM fields since they are electrically neutral.

Unlike electromagnetic plasmas, scatterings in QGP among quarks, antiquarks, and gluons are dominated by QCD interactions, which are much stronger than the electromagnetic forces. Therefore, response in the quark and antiquark distribution functions to EM fields can be treated as small corrections to the background distributions,

$$f_q = \bar{f}_q + \delta f_q, \qquad f_{\bar{q}} = \bar{f}_{\bar{q}} + \delta f_{\bar{q}}. \tag{3}$$

As a consequence of the smallness of $\delta f_{q/\bar{q}}$, one could treat the background distributions of quark and antiquark $\bar{f}_{q/\bar{q}}$ as being entirely determined by QCD interactions, so they are solutions to the Boltzmann equations:

$$p^\mu \partial_\mu \bar{f}_{q/\bar{q}} = \mathcal{C}[f_{q/\bar{q}}, f_g]. \tag{4}$$

Due to the charge conjugation symmetry of QCD, one has $\bar{f}_q = \bar{f}_{\bar{q}}$ and whence $h_q = \delta f_q - \delta f_{\bar{q}}$.

We now examine the condition $\delta f_{q/\bar{q}} \ll \bar{f}_{q/\bar{q}}$. By substituting Eq. (3) into Eq. (1b), one obtains an equation for $\delta f_{q/\bar{q}}$,

$$p^\mu \partial_\mu \delta f_{q/\bar{q}} + eQ_{q/\bar{q}} p_\mu F^{\mu\nu}\partial_{p^\nu}(\bar{f}_{q/\bar{q}} + \delta f_{q/\bar{q}}) = \mathcal{C}'[\delta f_{q/\bar{q}}], \tag{5}$$

where the collision kernel is deduced from the QCD interactions and is linear in $\delta f_{q/\bar{q}}$. The left-hand side of the equation reads parameterically: $\delta f_{q/\bar{q}}\Lambda_c^2 + \bar{f}_{q/\bar{q}}|eB|$, with Λ_c a characteristic energy scale introduced from the kinematic term. To the leading order in α_s, the collision term is further suppressed by α_s^2, giving rise to $\alpha_s^2\Lambda_c^2\delta f_{q/\bar{q}}$. Therefore, one finds $\delta f_{q/\bar{q}} \sim \bar{f}_{q/\bar{q}}|eB|/\Lambda_c^2$, from which $\delta f_{q/\bar{q}} \ll \bar{f}_{q/\bar{q}}$ translates into the condition $|eB| \ll \Lambda_c^2$. Recall that at the top energies of RHIC and the LHC, at initial time the external magnetic field is estimated as $|eB| \sim m_\pi^2$ with m_π the pion mass, while the only characteristic energy scale Λ_c in QGP is determined by the saturation energy, which is $Q_s \sim 1$ GeV. As the system expands, both the magnetic field and the energy scale of the QGP medium decrease, but the condition $|eB| \ll \Lambda_c^2$ remains valid for a sufficiently long time. Eventually, the condition breaks down when the system approaches local thermal equilibrium and becomes describable by MHD. For such a system, multiple energy scales emerge, including a typical hard energy scale corresponding to temperature T and a soft energy scale corresponding to spatial gradient ∇, and $|eB| \gg T\nabla$ [30,31]. More detailed discussions on the separation of scales will be given in Sec. III.

Given $\delta f_{q/\bar{q}} \ll \bar{f}_{q/\bar{q}}$, for each flavor, the splitting distribution can be shown approximately satisfying a collisionless Boltzmann-Vlasov equation,

$$p^\mu \partial_\mu h_q + 2eQ_q p_\mu F^{\mu\nu}\partial_{p^\nu}\bar{f}_q = 0, \tag{6}$$

where the Coulomb-Lorentz force is dominated by the leading order mean-field effect, i.e., the drifting of the background quarks and anti-quarks in the EM fields. With regards to Eq. (6), the charge carriers of the system that are coupled to the dynamical evolution of the EM fields are effectively the splittings between quarks and anti-quarks. For the leading order analysis, collisions are neglected as they are suppressed by α_s^2 in comparison to the Coulomb-Lorentz force. In an alternative aspect, the collisionless approximation is also supported by the fact that the frequency of the charge carriers, $\sim\Lambda_c$, is much greater than that from collisions, which is $\sim\alpha_s^2|eB|/\Lambda_c$ [32]. Note that the collisionless approximation should be recognized as a consequence subject to the condition $|eB| \ll \Lambda_c^2$, namely, when the system is far away from equilibrium. For a system close to local equilibrium, neglecting the collisions would give rise to infinite conductivity in QGP, which is apparently nonphysical. Accordingly, while the background distributions of quarks and antiquarks can be solved independently from Eq. (4), the couplings between the EM fields and the preequilibrium evolution of QGP are characterized by Eq. (1a) and Eq. (6).

In high-energy heavy-ion collisions, in the absence of the EM fields, the preequilibrium evolution of QGP can be well approximated with respect to the Bjorken symmetry [33].

That is to say, the background distribution of quarks and antiquarks are boost invariant along the beam axis (we refer to as the z axis) and translationally invariant in the transverse plane ($\mathbf{x}_\perp$). Corresponding to realistic heavy-ion collisions, this approximation applies to the $\mathbf{x}_\perp \sim 0$ region in collisions that are not too peripheral.

For the QCD interactions, we consider 2-to-2 elastic scatterings among massless up-quarks, down-quarks, and gluons: $q\bar{q} \leftrightarrow gg, qg \leftrightarrow qg, \bar{q}g \leftrightarrow \bar{q}g, gg \leftrightarrow gg$, at small angle approximation [34]. We are allowed to vary the strong coupling constant in these scatterings when solving the equation, for which we shall choose as $\alpha_s \sim 0.2$. The inelastic collisions are not included since, at the very early stages as we are focusing on, they are expected subdominant [35], which thereby would not significantly change the results we find in the current work. Nevertheless, the role of inelastic collisions on the EM fields is an interesting topic to investigate, which we leave for future studies. More details on solving the background quark and antiquark distributions can be found in Refs. [36,37], and Ref. [38] for a recent application to the computations of electromagnetic probes.

In heavy-ion collisions, the magnetic fields on average are perpendicular to the reaction plane, which we set to be along the y direction. In the reaction plane, there exist electric fields which are induced partly by the decay of the magnetic field and partly by the moving spectators. In accordance with this geometrical configuration, we choose the following gauge potential,

$$A^\mu = A^\mu_{\rm ex} + A^\mu_{\rm ind} = (0, A^x_{\rm ex}(t,z) + A^x_{\rm ind}(t,z), 0, 0), \quad (7)$$

which satisfies the Lorentz gauge condition $\partial_\mu A^\mu = 0$. Correspondingly, the independent EM-field components are given by

$$E^x(t,z) = -\partial_t A^x(t,z), \qquad B^y(t,z) = \partial_z A^x(t,z). \quad (8)$$

In Eq. (8), translational invariance in the transverse plane is implicitly assumed in analogous to the background QGP, which again makes our calculation mostly applicable at the central region of the transverse plane.

The external EM fields generated by the spectator nucleons have been extensively studied. Near $\mathbf{x}_\perp \sim \mathbf{0}$ they can be well expressed via effectively a Lienard-Wiechert potential [39,40]

$$A^x_{\rm ex}(t,z) = A_0 \left\{ \frac{z+vt}{[b^2/4 + \gamma^2(z+vt)^2]^{1/2}} + \frac{z-vt}{[b^2/4 + \gamma^2(z-vt)^2]^{1/2}} \right\}, \quad (9)$$

where b is the impact parameter, $v = \sqrt{1-(2m/\sqrt{s})^2}$ is the velocity of the nucleus, and $\gamma = 1/\sqrt{1-v^2}$. A_0 is a constant parameter to specify the colliding systems, which depends on the atomic number of the colliding nucleus. The external EM fields evolve independently and satisfy by themselves the Maxwell equation, corresponding to which is the external charged current $j^\mu_{\rm ex}$. Accordingly, the Maxwell equation for the induced fields reduces to

$$(\partial_t^2 - \partial_z^2) A^x_{\rm ind} = -\partial_t E^x_{\rm ind} - \partial_z B^y_{\rm ind} = j^x_{\rm ind}, \quad (10)$$

with $j^x_{\rm ind}$ being given in Eq. (2).

III. SEPARATION OF SCALES IN PREEQUILIBRIUM QGP

To verify the separation of scales in the coupled system of preequilibrium QGP and EM fields, we present here parametric descriptions of the evolution of these corresponding scales, $|eB|$ and $T\nabla$.

The approaching to local thermal equilibrium of the QGP in the very early stages of heavy-ion collisions can be well captured by Bjorken expansion of interacting quarks and gluons, where the longitudinal expansion and scatterings among the quarks and gluons are two competing effects, driving the system towards free streaming and ideal fluidity, respectively.

Although the QGP system created via nucleus-nucleus collisions differs from event to event, how its energy density decay follows an universal solution known as the attracor. For illustrative purposes, we define the relative decay rate of the energy density,

$$g(t) \equiv \frac{t}{\varepsilon}\frac{d\varepsilon}{dt} \to \varepsilon(t) \sim t^{g(t)}, \quad (11)$$

for which the properties of the attractor are well known (cf. Refs. [41,42]),

(i) For a conformal system as we are considering, positiveness of the pressures along longitudinal and transverse directions leads to constraints on the relative decay rate of the energy density, $g(t) \in [-2,-1]$, where the two extremes correspond to the cases of vanishing transverse pressure and longitudinal pressure, respectively.

(ii) With respect to the QGP medium that evolves from the free streaming to ideal fluidity, attractor solution of $g(t)$ is a smooth transition from $g(t) = -1$ at very early times to $g(t) = -4/3$ at late times, irrespective of the details of interaction among quarks and gluons. Here, $g(t) = -1$ is a stable fixed point of free streaming while $g(t) = -4/3$ is the pseudo-fixed point corresponding to the ideal hydrodynamic evolution.

For arbitrary evolutions, although $g(t)$ may be randomly initialized between -2 and -1, it merges to the attractor solution when effects of interactions become comparable to

the longitudinal expansion, and evolves towards to $-4/3$ at late times.

It has been shown from our numerical solutions, that the magnetic field evolves from t^{-3} decay at early times, and approaches to t^{-1} decay eventually. These are actually decay patterns correspond to the external magnetic field created by (dominantly) the spectators of nucleus-nucleus collisions, and ideal MHD, respectively. Since the external field evolution and induction from the QGP medium are the two competing contributions to the magnetic field, t^{-3} decay and t^{-1} should be recognized as the two extremes of the observed behavior of the magnetic field. In general, one thus has

$$\frac{t}{|eB|}\frac{d|eB|}{dt} \in [-3,-1]. \tag{12}$$

Moreover, in analogous to the attractor picture of QGP hydrodynamization, one may expect some universal evolution pattern of the magnetic field whose decay rate connects -3 from early times to -1 at late times, with negligible dependence on the details of medium interactions.

Since $T \sim \varepsilon^{1/4}$ and the gradient of the Bjorken expanding medium is $\nabla \sim 1/t$, the characteristic energy scale in the QGP medium $T\nabla$ can be related to $g(t)$ as $T\nabla \sim t^{g(t)/4-1}$. Correspondingly, the relative decay rate of $T\nabla$ must satisfy,

$$\frac{g(t)}{4} - 1 \in \left[-\frac{3}{2}, -\frac{5}{4}\right], \tag{13}$$

which is slower than the early-time decay rate of the magnetic field, $|eB| \sim t^{-3}$. It is only at late times, when the evolution of the magnetic field becomes describable by ideal MHD, that $|eB| \sim t^{-1}$, can one realize a faster decay of ∇T than $|eB|$. Therefore, accounting for also the initial scale separation $T\nabla \sim Q_s^2 \gg |eB| \sim m_\pi^2$, and taking the fastest decay of $T\nabla$ ($\sim t^{-3/2}$) and the slowest decay of the magnetic field ($\sim t^{-1}$), an estimate can be obtained that the scale separation cannot be violated before time t_s,

$$t_s \sim (Q_s^2/m_\pi^2)^2 t_0. \tag{14}$$

As an illustration, Fig. 1 depicts the evolution behavior of $|eB|$ and $T\nabla$ from our numerical solutions of AuAu collision with initial quarks. A smooth transition between the early-time t^{-3} decay and late-time t^{-1} decay in the evolution of $|eB|$ (blue solid line) is observed. In this particular event, the early-time decay of energy density differs from free streaming with $g(t) \approx -1.28$, which leads to the relative decay rate of $T\nabla$ as -1.32. Onset of ideal hydrodynamics has not yet been achieved during the calculations, with the decay of $T\nabla$ approaches -1.27 at $t \sim 8/Q_s$. Nonetheless, at the later stages, a faster decay of $T\nabla$ than $|eB|$ is realized, but the scale separation is still obvious.

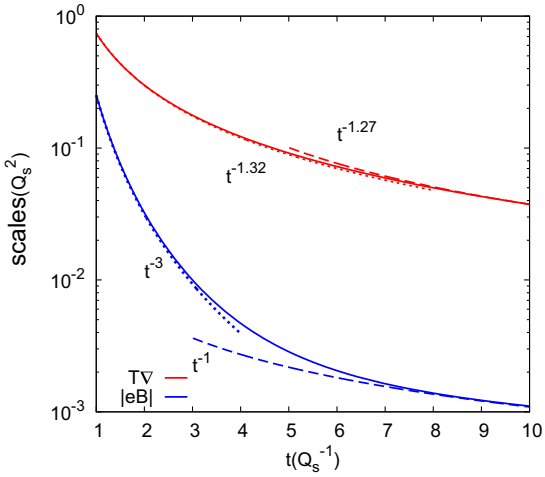

FIG. 1. Evolution of $|eB|$ (blue solid line) and $T\nabla \sim \varepsilon^{1/4}/t$ (red solid line) in AuAu collisions with initial quarks, where ε is the energy density. The dashed lines and dotted lines indicate, respectively, early-time and late-time decay patterns.

IV. EVOLUTION OF MAGNETIC FIELD

With the above setup, we are able to solve the time evolution of both the QGP and the EM fields for given initial conditions. We take an initial condition for the gluon and quark distribution functions inspired by the saturation physics [43]:

$$f_{g/q/\bar{q}}(t_0, z=0, \mathbf{p}) = f^{(0)}_{g/q/\bar{q}}\theta\left(1 - \frac{\sqrt{p_z^2\xi^2 + \mathbf{p}_\perp^2}}{Q_s}\right). \tag{15}$$

Parameters in the initial condition will be taken according to the same strategy as in Ref. [38], namely, to be determined with respect to the multiplicity yields in realistic heavy-ion collisions. For instance, for the parameter ξ which initializes the QGP out-of-equilibrium, we only consider the case $\xi = 1.4$, accounting for the effects of attractor solutions (cf. Ref. [41] and Ref. [42] for a recent review). We choose the saturation scale $Q_s = 1$ GeV, and accordingly we set $t_0 = 1Q_s^{-1} \sim 0.2$ fm/c as the initial time of the system evolution. The constants $f^{(0)}_{q/\bar{q}}$ and $f^{(0)}_g$ specify the occupation of quarks and gluons at initial time. Except the constraint $f^{(0)}_{q/\bar{q}} \leq 1$ from Pauli exclusion principle, initial quark occupation should be further determined by the study of quark production before the kinetic regime through, e.g., the Schwinger mechanism in classical gluon fields [44–48]. In this work, we consider two limiting cases: Without initial quarks with $f^{(0)}_{q/\bar{q}} = 0$ and quarks are fully populated initially with $f^{(0)}_{q/\bar{q}} = 1$. The initial gluon occupation $f^{(0)}_g$ is then determined to reproduce the multiplicity yields in the 20%–30% centrality class of

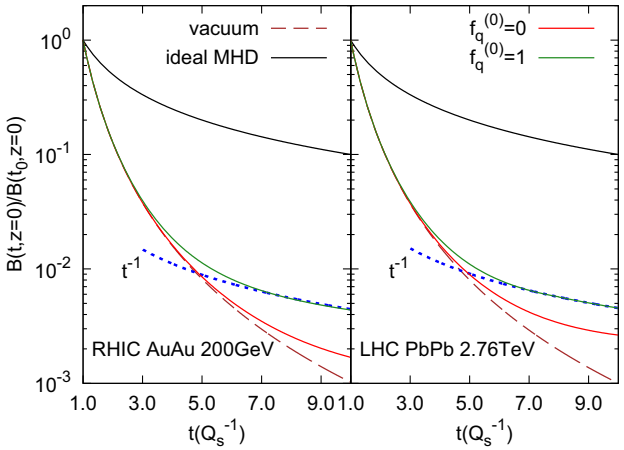

FIG. 2. Evolution of the magnetic field at $z = 0$ for the AuAu collisions at RHIC (left) and PbPb collisions at the LHC (right), relative to its initial strength at $t = t_0$. In comparison to the decay of the magnetic field in vacuum (brown dashed lines), effects due to the QGP medium with initial quarks (red solid lines) and without initial quarks (green solid lines) are obvious. The expected t^{-1} decay from ideal MHD is plotted as the black solid lines and blue dotted lines.

AuAu collisions at RHIC with $\sqrt{s_{NN}} = 200$ GeV [49] and PbPb collisions at LHC with $\sqrt{s_{NN}} = 2.76$ TeV [50].

With all these parameters given, we can solve the coupled differential equations numerically. Results shown in Fig. 2 are the time evolution of the magnetic field relative to its initial value at $z = 0$, i.e., the center in the QGP medium, for AuAu collisions at RHIC and PbPb collisions at the LHC. For comparison, we also present the results of two extreme scenarios in which analytical solutions exist. The first is the evolution of the magnetic field in vacuum, where the decay of magnetic field is entirely determined by the spectator nucleons moving relativisticly, resulting a time dependence $\sim t^{-3}$ [40]. This is exactly the evolution of the external field in our study. The second corresponds to solutions of ideal MHD, with regard to an infinite electric conductivity $\sigma \to \infty$. The evolution of the magnetic field is then determined by the magnetic flux conservation in the conducting QGP. For the Bjorken expansion it is estimated as $\sim t^{-1}$ [4,25]. For more realistic heavy-ion collisions, as a consequence of the QGP evolving towards local equilibrium, the evolution of the magnetic field interpolates these two limits. For example, for the solution with respect to $f_q^{(0)} = 1$ (green lines in Fig. 2), the magnetic field starts following the vacuum solution t^{-3}, then tends to behave $\sim t^{-1}$ at late times. Deviations from the vacuum solutions are those generated from induction.

In analogous to the hydrodynamization process characterized by the evolution of energy density in a preequilibrium QGP (cf. Ref. [27]), the evolution of the magnetic field can be used to monitor the onset of MHD. However, the evolution of the magnetic field is more involved as it reflects not only the dynamical aspect of the QGP, but also depends on its chemical evolution. Initially, irrespective to quark occupation, QGP is dominated by gluon saturation, which leads to approximately a charge neutral medium that barely couples to the EM fields, so it explains the t^{-3} behavior at early times. As the system evolves towards chemical equilibrium with quarks generated gradually via scatterings, the medium becomes more and more conducting and eventually evolves according to the MHD description. In particular, the t^{-1}-decay of the magnetic field is characteristic in ideal MHD in the Bjorken flow, hence it is the final and the *slowest* decay pattern of the magnetic field. However, from our simulations the t^{-1}-decay of the magnetic field emerges much earlier than the applicability of MHD when the coupled system is still out of equilibrium, a phenomenon that is also observed in the collisionless electromagnetic plasmas [32]. Of course, the condition $|eB| \gg T\nabla$ for local equilibrium and MHD should eventually be realized at later times, because $T\nabla \sim t^{-4/3}$ decays faster than the magnetic field. Comparing to a system initialized purely by gluons, chemical equilibrium in the QGP is more easily realized when quarks are populated initially, which explains in Fig. 2 the slower decay of magnetic field in QGP with initial quarks than that without initial quarks.

Although the effects of induction from the out-of-equilibrium QGP are comparable at RHIC and LHC, as being recognized from the relative decay in Fig. 2, the absolute strength of the magnetic field is much stronger at RHIC. This is because the field strength relies, to a larger extent, on its external field component. Shown in Fig. 3, are the magnetic fields along the z axis, plotted in units of pion

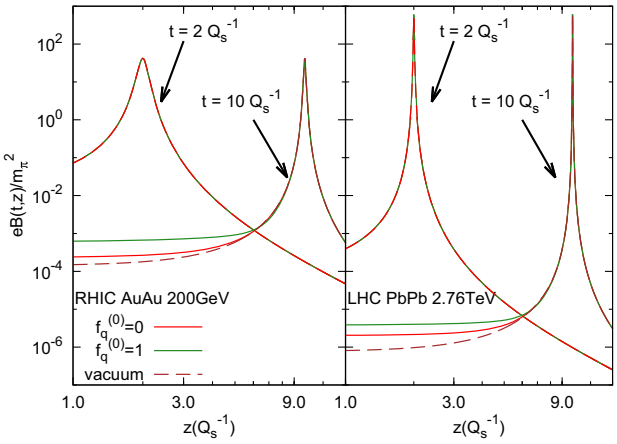

FIG. 3. Distribution of the magnetic field along the z axis at $t = 2Q_s^{-1}$ and $t = 10Q_s^{-1}$, in units of m_π^2, for AuAu collisions at $\sqrt{s_{\rm NN}} = 200$ GeV (left) and PbPb at $\sqrt{s_{\rm NN}} = 2.76$ TeV (right). Numerical solutions with respect to QGP medium initialized with $f_q^{(0)} = 0$ and $f_q^{(0)} = 1$ are plotted as red solid lines and green solid lines, respectively. For comparison, the distributions of the magnetic field in vacuum are shown as brown dashed lines.

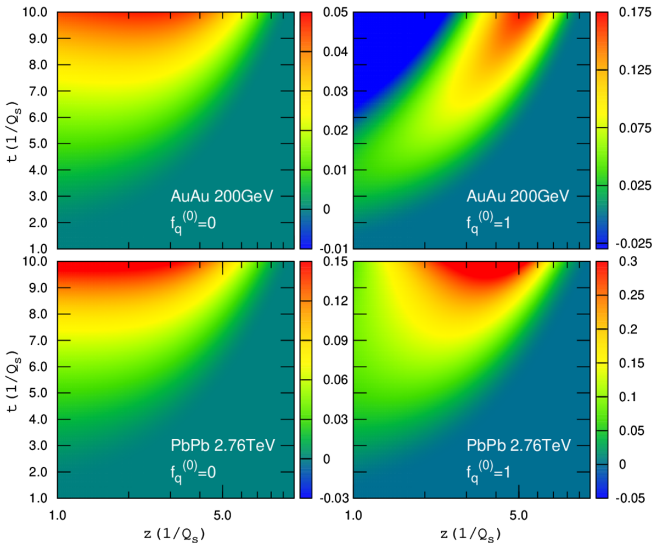

FIG. 4. The ratio $j^x_{\rm ind}/E^x$ from AuAu collisions at $\sqrt{s_{\rm NN}} =$ 200 GeV (up) and PbPb at $\sqrt{s_{\rm NN}} = 2.76$ TeV (down), with initial quarks (right) and without initial quarks (left), in unit of Q_s.

mass square, at $t = 2Q_s^{-1}$ and $10Q_s^{-1}$. We emphasize that at $t = 10Q_s^{-1} \sim 2$ fm/c, the QGP system is expected to evolve hydrodynamically, yet it may be not fully equilibrated [28,36]. The peaks of these distributions point to the positions of the colliding nuclei at the respective instants. Again, an induced magnetic field can be noticed as the difference between the vacuum solution and the solution with respect to QGP, which, as expected, only becomes significant at late times and in the spatial area where the QGP medium exists. The critical scales in a QGP medium correspond to the mass of light quarks, $(m_q/m_\pi)^2 \sim 10^{-4}$, and temperature $(T/m_\pi)^2 \sim (\Lambda_{\rm QCD}/m_\pi)^2$. In comparison to these scales, we found, by the time the QGP starts to evolve hydrodynamically, the residual strength of the magnetic field satisfies the hierarchy, $(m_q/m_\pi)^2 \ll |eB|/m_\pi^2 \ll (T/m_\pi)^2$ at RHIC, but can be negligible at the LHC. This is possibly the reason why CME has not been detected at the LHC experiments [51].

Figure 4 presents the ratio $j^x_{\rm ind}/E^x$ at the RHIC and the LHC collisions, in units of $Q_s = 1$ GeV. The purpose of studying this ratio is twofold. First, as a straightforward generalization of the electric conductivity to systems out of equilibrium, $j^x_{\rm ind}/E^x$ characterizes the conducting ability of the QGP during its preequilibrium stages. Note, however, due to the influence of the magnetic fields on the QGP medium, one should not simply identify the ratio to the electric conductivity. Since the background QGP experiences Bjorken expansion, the ratio is nonzero only in the region with $z < t$. As shown in Fig. 4, the QGP becomes more conducting as it evolves towards equilibrium, reflecting the continuous quark and antiquark production, in consistency with what we have learned before.

Secondly, $j^x_{\rm ind}$ signifies the motion of charged particles in the reaction plane due to the presence of EM fields. It gives, in particular, one major origin of the charge dependent flow v_1 observed in experiments [52,53]. Importantly, the induced current contains contributions from both the electric and the magnetic fields, but in opposite directions: $j^x_{\rm ind} \propto E^x - v_z B^y$. These distinct field components are relevant to the rapidity dependence of the observed v_1 [16,23,54,55],[1] whose relative significance can be investigated in term of the sign of $j^x_{\rm ind}/E^x$. For all the cases we are considering, the induced current is dominated by the electric field component, thus $j^x_{\rm ind}/E^x > 0$. However, an exception $j^x_{\rm ind}/E^x < 0$ is observed in the central region at the RHIC AuAu collisions when initially quarks are fully populated (top-right panel). Here the dominant effect comes from the magnetic field. It is worth mentioning that, couplings to EM fields are more substantial for the transport of heavy-flavor quarks, leading to a more significant effect. Nonetheless, the preequilibrium motion of charged particles due to the EM fields does not seem to be consistent with the observed sign change of heavy flavor v_1 from RHIC to the LHC experiments.

V. SUMMARY AND DISCUSSION

We have presented the evolution of magnetic field in the preequilibrium stages of the QGP for realistic heavy-ion collisions, from the numerical solutions to the coupled Boltzmann-Vlasov equation and Maxwell equations. We showed that the electric induction in QGP slows down the decay of magnetic field and found that the residual strength of the magnetic field after preequilibrium evolution is still strong at RHIC in comparison to the critical scale given by light quark mass, but negligible at the LHC. We found that the evolution of the magnetic field approaches the description of an ideal MHD, namely, t^{-1} decay, at later times, although the applicability condition $|eB| \gg T\nabla$ for MHD has not been achieved. We also studied the ratio $j^x_{\rm ind}/E^x$, which is in general dominated by its electric field component. However, when the effect of the magnetic field is enhanced such as in the RHIC collisions with initial-state quarks, the induced charged current follows the direction determined by the magnetic field. Our findings can provide initial input for MHD simulations for heavy-ion collisions and may also underlie the quantitative computations of the magnetic-field induced observables like the CME signal and the charge-dependent directed flow of heavy flavors.

[1]Note that the orientations of the electromagnetic fields in this work are opposite to those considered by experiments (cf. Refs. [52,53]), for the positively charged hadrons, the electric field can lead to $dv_1(y)/dy < 0$, while the magnetic field tends to drive $dv_1(y)/dy > 0$.

ACKNOWLEDGMENTS

X.-G. H. is supported by NSFC through Grant No. 12075061 and Shanghai NSF through Grant No. 20ZR1404100. L. Y. is supported by the NSFC Grants through No. 11975079 and by Shanghai Pujiang Program (No. 19PJ1401400).

[1] V. Skokov, A. Y. Illarionov, and V. Toneev, Int. J. Mod. Phys. A **24**, 5925 (2009).
[2] A. Bzdak and V. Skokov, Phys. Lett. B **710**, 171 (2012).
[3] V. Voronyuk, V. D. Toneev, W. Cassing, E. L. Bratkovskaya, V. P. Konchakovski, and S. A. Voloshin, Phys. Rev. C **83**, 054911 (2011).
[4] W.-T. Deng and X.-G. Huang, Phys. Rev. C **85**, 044907 (2012).
[5] J. Bloczynski, X.-G. Huang, X. Zhang, and J. Liao, Phys. Lett. B **718**, 1529 (2013).
[6] D. E. Kharzeev, L. D. McLerran, and H. J. Warringa, Nucl. Phys. **A803**, 227 (2008).
[7] K. Fukushima, D. E. Kharzeev, and H. J. Warringa, Phys. Rev. D **78**, 074033 (2008).
[8] Y. Burnier, D. E. Kharzeev, J. Liao, and H.-U. Yee, Phys. Rev. Lett. **107**, 052303 (2011).
[9] K. Tuchin, Phys. Rev. C **82**, 034904 (2010); **83**, 039903(E) (2011).
[10] G. Basar, D. Kharzeev, D. Kharzeev, and V. Skokov, Phys. Rev. Lett. **109**, 202303 (2012).
[11] G. S. Bali, F. Bruckmann, G. Endrodi, and A. Schafer, Phys. Rev. Lett. **112**, 042301 (2014).
[12] K. Tuchin, Phys. Rev. C **91**, 014902 (2015).
[13] G. Cao and X.-G. Huang, Phys. Lett. B **757**, 1 (2016).
[14] K. Fukushima, K. Hattori, H.-U. Yee, and Y. Yin, Phys. Rev. D **93**, 074028 (2016).
[15] X. Guo, S. Shi, N. Xu, Z. Xu, and P. Zhuang, Phys. Lett. B **751**, 215 (2015).
[16] S. K. Das, S. Plumari, S. Chatterjee, J. Alam, F. Scardina, and V. Greco, Phys. Lett. B **768**, 260 (2017).
[17] N. Sadooghi and F. Taghinavaz, Ann. Phys. (Amsterdam) **376**, 218 (2017).
[18] K. Fukushima and Y. Hidaka, Phys. Rev. Lett. **117**, 102301 (2016).
[19] L. McLerran and V. Skokov, Nucl. Phys. **A929**, 184 (2014).
[20] K. Tuchin, Phys. Rev. C **88**, 024911 (2013).
[21] H. Li, X.-l. Sheng, and Q. Wang, Phys. Rev. C **94**, 044903 (2016).
[22] U. Gursoy, D. Kharzeev, and K. Rajagopal, Phys. Rev. C **89**, 054905 (2014).
[23] U. Gürsoy, D. Kharzeev, E. Marcus, K. Rajagopal, and C. Shen, Phys. Rev. C **98**, 055201 (2018).
[24] G. Inghirami, L. Del Zanna, A. Beraudo, M. H. Moghaddam, F. Becattini, and M. Bleicher, Eur. Phys. J. C **76**, 659 (2016).
[25] V. Roy, S. Pu, L. Rezzolla, and D. Rischke, Phys. Lett. B **750**, 45 (2015).
[26] V. Roy, S. Pu, L. Rezzolla, and D. H. Rischke, Phys. Rev. C **96**, 054909 (2017).
[27] A. Kurkela and Y. Zhu, Phys. Rev. Lett. **115**, 182301 (2015).
[28] A. Kurkela, A. Mazeliauskas, J.-F. Paquet, S. Schlichting, and D. Teaney, Phys. Rev. C **99**, 034910 (2019).
[29] J. Berges, M. P. Heller, A. Mazeliauskas, and R. Venugopalan, Rev. Mod. Phys. **93**, 035003 (2021).
[30] L. D. Landau, E. M. Lifshitz, and L. P. Pitaevskii, *Electrodynamics of Continuous Media*, Course of Theoretical Physics (Butterworth, Oxford, 1984).
[31] J. Hernandez and P. Kovtun, J. High Energy Phys. 05 (2017) 001.
[32] E. M. Lifshitz and L. P. Pitaevskii, *Physical Kinetics, Course of Theoretical Physics* (Pergamon, Oxford, 1981).
[33] J. D. Bjorken, Phys. Rev. D **27**, 140 (1983).
[34] J.-P. Blaizot, B. Wu, and L. Yan, Nucl. Phys. **A930**, 139 (2014).
[35] R. Baier, A. H. Mueller, D. Schiff, and D. T. Son, Phys. Lett. B **502**, 51 (2001).
[36] J.-P. Blaizot and L. Yan, J. High Energy Phys. 11 (2017) 161.
[37] N. Tanji and R. Venugopalan, Phys. Rev. D **95**, 094009 (2017).
[38] J. Churchill, L. Yan, S. Jeon, and C. Gale, Phys. Rev. C **103**, 024904 (2021).
[39] X.-G. Huang, Rep. Prog. Phys. **79**, 076302 (2016).
[40] K. Hattori and X.-G. Huang, Nucl. Sci. Tech. **28**, 26 (2017).
[41] P. Romatschke, Phys. Rev. Lett. **120**, 012301 (2018).
[42] C. Shen and L. Yan, Nucl. Sci. Tech. **31**, 122 (2020).
[43] P. Romatschke and M. Strickland, Phys. Rev. D **68**, 036004 (2003).
[44] M. Gyulassy and A. Iwazaki, Phys. Lett. **165B**, 157 (1985).
[45] G. C. Nayak, Phys. Rev. D **72**, 125010 (2005).
[46] N. Tanji, Ann. Phys. (Amsterdam) **325**, 2018 (2010).
[47] R. Ryblewski and W. Florkowski, Phys. Rev. D **88**, 034028 (2013).
[48] M. Ruggieri, A. Puglisi, L. Oliva, S. Plumari, F. Scardina, and V. Greco, Phys. Rev. C **92**, 064904 (2015).
[49] S. S. Adler *et al.* (PHENIX Collaboration), Phys. Rev. C **71**, 034908 (2005); **71**, 049901(E) (2005).
[50] S. Chatrchyan *et al.* (CMS Collaboration), Phys. Rev. Lett. **109**, 152303 (2012).
[51] V. Khachatryan *et al.* (CMS Collaboration), Phys. Rev. Lett. **118**, 122301 (2017).
[52] J. Adam *et al.* (STAR Collaboration), Phys. Rev. Lett. **123**, 162301 (2019).
[53] S. Acharya *et al.* (ALICE Collaboration), Phys. Rev. Lett. **125**, 022301 (2020).
[54] J.-J. Zhang, X.-L. Sheng, S. Pu, J.-N. Chen, G.-L. Peng, J.-G. Wang, and Q. Wang, Phys. Rev. Res. **4**, 033138 (2022).
[55] L. Oliva, S. Plumari, and V. Greco, J. High Energy Phys. 05 (2021) 034.